CHROMATICITY AND WAKE FIELD EFFECT ON THE TRANSVERSE MOTION OF LONGITUDINAL BUNCH SLICES IN THE TEVATRON

FERMILAB-PUB-07-448-AD

V. H. Ranjbar, P. Ivanov,
Fermilab, Batavia, IL
(Dated: November 13, 2007)

The Transverse turn-by-turn evolution of a bunch slice after an impulse kick is examined considering chromatic and impedance effects. It is found that by fitting the envelope of the beam slice motion to simulated data is consistent with a resistive wall wake field the strength of which can be determined by fitting.

PACS numbers:

I. INTRODUCTION

The Tevatron Run II project seeks to deliver 1.96 TeV center of mass proton-antiproton collisions to experiments CDF and D0 located at two collision points in the Tevatron ring. The process begins with the production of protons which are accelerated through four stages beginning with a 400 MeV linac, 8 GeV Booster, 150 GeV Main Injector and final acceleration in the Tevatron to 980 GeV. Prior to this protons are extracted from Main Injector and fired against a tungsten target to produce antiprotons which are then transported and cooled in the Debuncher and further cooled and accumulated in the Accumulator and Recycler. After enough cooled antiprotons have been accumulated for a Tevatron store both species are then accelerated to collision energy of 980 GeV.

In order to deliver as many collisions as possible to the experiments non-luminous proton and antiproton losses need to be reduced as much as possible. One significant source of continuous loss is related to head-tail instabilities driven by wake fields. These instabilities require running the Tevatron with a large chromaticity at High Energy Physics store. High chromaticities however increase the total tune spread and reduce beam lifetime by increasing the likelihood that a particle will cross a resonant tune value and either be lost or have its action increased.

Clearly an understanding of this head-tail instability and the evolution of the bunch is important if we seek to run the Tevatron with a lower chromaticity and ways to counteract losses are sought. Improvements in the speed of available digital oscilloscopes now make it possible to experimentally measure the transverse evolution of longitudinal bunch slices down to resolutions below .4 ns. It is now possible to directly compare existing or new models with experiment and arrive at a more exact characterization of the collective transverse motion of a single coalesced bunch in the Tevatron.

As a result of previous efforts to understand the source and magnitude of the impedance in the Tevatron based on the analysis of data obtained from this new breed of fast digital oscilloscopes improvements have been made to bring down the effective impedance from $5M\Omega/m$ to now $1M\Omega/m$ [1]-[2]. The analysis was based primarily on the basis of instability growth rate and comparison with simulation.

In this paper we present a systematic approach where a careful comparison between simulation and measurement allows one to fit the transverse wake field by fitting the observable deformation of the transverse bunch profiles. This allows for the development of a new approach to estimate the strength and likely structure of the short range wakefield by comparison with a model with only three relevant parameters. Two of these parameters, linear and 2nd order chromaticity are independently measurable leaving only the strength and structure of the wake field to be determined from a fit.

II. EXPERIMENTAL SET-UP

Using the 1 meter long strip line detector installed at F0 in the Tevatron the signal was captured using a Tektronixs Digital Phosphorus TDS7154 oscilloscope. The A-B and A+B signals were measured in fast-frame mode with a resolution of 0.4 ns across an 8 ns frame for 1000-2000 turns. The set-up can be seen in Fig. 1. Since the recorded signal was the sum the image current traveling with the beam and the reflected image of the beam from the downstream end we first reconstructed the single image by subtracting out the reflected image. This was accomplished using knowledge of the length of strip line and the velocity of the beam. Reconstruction can be accomplished either digitally or in an analog fashion by delaying and re-summing the signals in the appropriate manner. After reconstruction of the signal the transverse position could then be evaluated using,

$$Z(n,\tau) = E\frac{(A(n,\tau) - B(n,\tau))}{(A(n,\tau) + B(n,\tau))}. \quad (1)$$

Here E a geometric factor from the angular width of the stripline, n the turn number and τ the longitudinal slice.

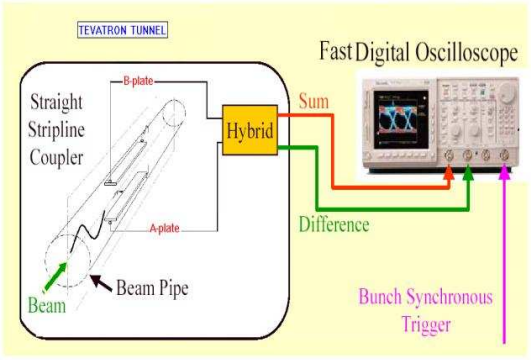

FIG. 1: Experimental Set-up

III. COMPARISON WITH A SIMPLE ANALYTICAL MODEL

In the simplest case a single particle's transverse motion can be characterized by

$$\frac{d^2Y(s)}{ds^2} + \omega_\beta^2/c^2 Y(s) \;=\; 0. \tag{2}$$

Here Y is the transverse position of the particle, s the longitudinal coordinate and ω_β gives the angular betatron frequency, which is just the angular revolution frequency ω_0 times Q the betatron tune. Solutions give transverse harmonic motion oscillating with the betatron tune Q each revolution. However if the particle resides in a rf-bucket one must consider its longitudinal motion inside of the bucket as well and equation of motions become,

$$\frac{d^2Y(s,\delta,z)}{ds^2} + \omega_\beta^2(\delta)/c^2 Y(s,\delta,z) \;=\; 0. \tag{3}$$

Here z defines the longitudinal position relative to the center of the rf-bucket, and $\delta = \Delta p/p$ the relative momentum difference from the "on momentum" particle. If we expand the betatron frequency to first order in δ we obtain.

$$\omega_\beta(\delta) = \omega_0 Q + \xi\omega_0\delta \tag{4}$$

Here ξ is called the chromaticity. We can also approximate the longitudinal motion inside the rf-bucket using,

$$\begin{aligned} \delta(s) &= \frac{-\omega_s}{\eta c} r\sin(\omega_s s/c + \phi) \\ z(s) &= r\cos(\omega_s s/c + \phi). \end{aligned} \tag{5}$$

Here $\omega_s = \omega_0 Q_s$ known as the synchrotron angular frequency is the angular frequency of the longitudinal motion, and ϕ is the phase of the synchrotron motion, η the slippage factor.

An approximate solution to Eq. (3) has the form,

$$Y(s,\delta,z) \approx Ae^{\pm i\Phi(s,\delta,z)} \tag{6}$$

where A is the constant amplitude and,

$$\begin{aligned} \Phi(s,\delta,z) &= \int_0^s ds'(\omega_0 Q/c + \omega_0\xi\delta(s)/c) \\ \Phi(s,\delta,z) &= \omega_0 Qs/c + \frac{\xi\omega_0}{\eta c}(z(s) - z(0)) \\ \Phi(s,\delta,z) &= \omega_0 Qs/c + \frac{\xi\omega_0 z}{\eta c}(1-\cos(\omega_s s/c)) + \\ \frac{\xi\delta}{Q_s}\sin(\omega_s s/c). \end{aligned} \tag{7}$$

Here we have assumed the particles kicked together are in phase with, $\Phi(0,\delta,z) = 0$. We have recast $z(0)$ in terms of $z(s)$ and $\delta(s)$ using the transformation from the frame rotating with the synchrotron frequency,

$$\begin{pmatrix} z(s) \\ \delta(s) \end{pmatrix} = \begin{pmatrix} \cos(\omega_s s/c) & \frac{\eta c}{\omega_s}\sin(\omega_s s/c) \\ -\frac{\omega_s}{\eta c}\sin(\omega_s s/c) & \cos(\omega_s s/c) \end{pmatrix} \begin{pmatrix} z(0) \\ \delta(0) \end{pmatrix}. \tag{8}$$

If we integrate Y over a Gaussian δ distribution $\rho(\delta) = \frac{e^{-\frac{\delta^2}{2\sigma_\delta^2}}}{\sqrt{2\pi}\sigma_\delta}$,we can obtain an expression for the transverse motion for a 'fixed' longitudinal slice

$$\mathrm{Re}\int_{-\infty}^{\infty} d\delta\rho(\delta)Y(s,\delta,z) = e^{-\frac{\chi^2}{2}\sigma_\tau^2\sin^2(\omega_s s/c)}\sin(\omega_0 Qs/c + \chi\tau(1-\cos(\omega_s s/c))). \tag{9}$$

Where we have defined a head-tail phase factor $\chi = \frac{\omega_0\xi}{\eta}$ and set $z = \tau c$ and assuming the τ and δ distributions are matched to the RF bucket we can use, $\sigma_\delta = \frac{\omega_s\sigma_\tau}{|\eta|}$. As can be seen in Fig. (2), the result yields collective motion with an envelope which de-coheres and re-coheres every 1/2 synchrotron period and a phase which de-coheres and

re-coheres every synchrotron period.

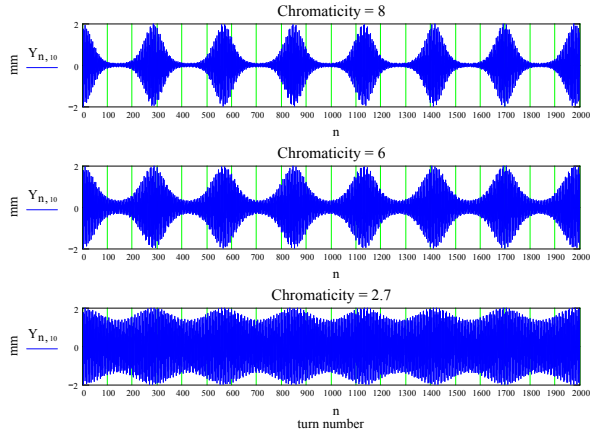

FIG. 2: Analytical model of transverse beam slice motion after 1 mm kick. With fixed rms bunch length σ_τ= 3 ns and decreasing chromaticity we can see the depth of the de-coherence envelope decrease

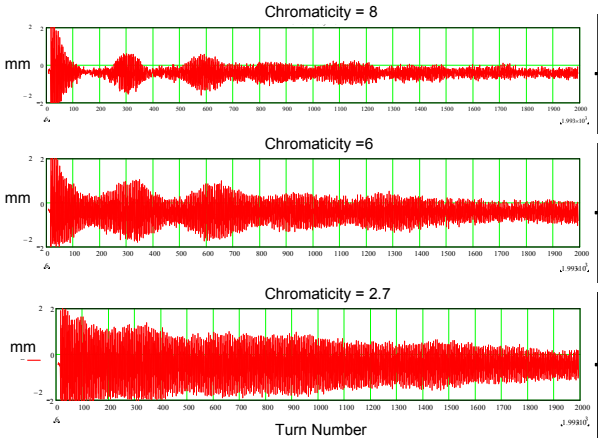

FIG. 3: Measured data of transverse beam slice motion after 1 mm kick. With fixed rms bunch length σ_τ= 3 ns and decreasing chromaticity we can see the depth of the de-coherence envelope decrease, comparable to simple analytical model.

A comparison with measured data in Fig. (3) from slices taken from the bunch center shows a similar coherence-de-coherence pattern with the strength of de-coherence correlating with the chromaticity. While this simple model captures many of the features of the transverse collective motion of the beam there are many other aspects of the motion which even a cursory comparison shows to be deficient. A comparison of the model with the actual beam motion in Fig. (4) reveals a difference in long term de-coherence and τ dependence.

Without too much difficulty this analysis can be taken a step further to include the effects of 2nd order Chromaticity ξ' again following [3], the betatron tune can be

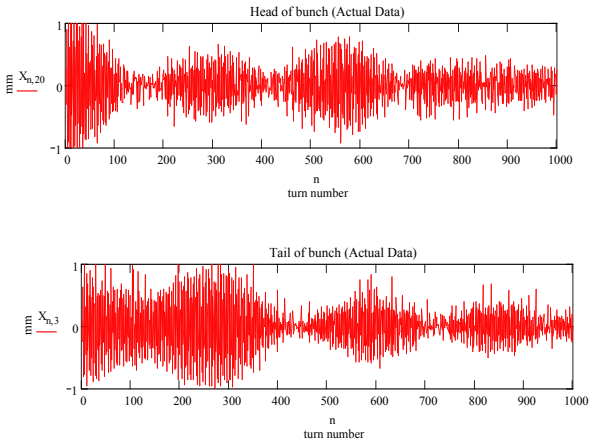

FIG. 4: Transverse beam motion after 1 mm kick with .4 nsec longitudinal bunch slices of Head (top) and the Tail (bottom) each 4 nsecs from the bucket center. Chromaticity measured to be $\xi = 4.0 \pm 1$ and σ_τ= 3 necs.

expanded to second order in δ

$$\omega_\beta(\delta) = \omega_0(Q + \xi\delta + \frac{1}{2}\xi'\delta^2). \tag{10}$$

The phase $\Phi(s, \delta, z)$ can be found by including the second order terms in the integral in Eq. (7). The result is the addition of three terms to Φ,

$$\frac{\omega_0\xi'\tau\delta}{4\eta}(1 - \cos(2\omega_s s/c)) + \frac{\omega_0\omega_s^2\xi'\tau^2}{4\eta^2}(s/c - \frac{\sin(2\omega_s s/c)}{2\omega_s}) + \frac{\omega_0\xi'\delta^2}{4}(s/c + \frac{\sin(2\omega_s s/c)}{2\omega_s}) \tag{11}$$

As with the first order case this equation can also be integrated over a Gaussian distribution analytically yielding,

$$
\begin{aligned}
\alpha(\tau,n) &= (\frac{\xi}{Q_s}\sin(2n\pi Q_s) + \frac{\omega_0\xi'}{4\eta}\tau(1-\cos(4n\pi Q_s)))\sigma_\delta \\
\theta(n) &= \pi\xi'\sigma_\delta^2\left(n + \frac{\sin(4n\pi Q_s)}{4\pi Q_s}\right) \\
\phi(\tau,n) &= \frac{\omega_0\xi}{\eta}\tau(1-\cos(2n\pi Q_s)) + \frac{\pi\omega_0^2 Q_s^2\xi'}{2\eta^2}\tau^2(n - \frac{\sin(4n\pi Q_s)}{4\pi Q_s}) - \frac{1}{2}\left(\frac{\alpha^2(\tau,n)\theta(n)}{1+\theta^2(n)} - \arctan(\theta(n))\right) \\
Y(\tau,n) &= \frac{e^{\frac{\alpha(\tau,n)^2}{2(1+\theta(n)^2)}}}{(1+\theta(n)^2))^{1/4}}\sin(2n\pi Q + \phi(\tau,n))
\end{aligned}
\tag{12}
$$

Here we have rescaled our time variable setting $s = nC$ where C is the circumference of the ring and n is the turn number. The inclusion of 2nd order Chromaticity shown in Fig. (5) reveals that we can capture the long term de-coherence and some aspects of the beam envelopes τ dependence. However, we can not explain a coherence-re-coherence, pattern, where a small re-coherence is followed by a large re-coherence. Since the remaining outstanding effect operates asymmetrically on the bunch we believe that this should be explained by the inclusion of wake fields. Other effects such as space charge and synchrotron tune spread while significant representing tune shifts on the order of 7×10^{-4} operate symmetrically on the bunch and therefore could not account for the behavior of the beam envelope.

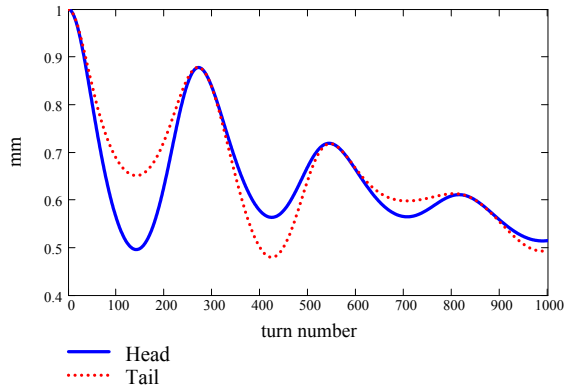

FIG. 5: Simulated transverse motion using analytical solution with first and second order chromaticity shown in Eq. (12). After 1 mm kick with .4 ns longitudinal bunch slices of Head (solid trace) and the Tail (dotted) each 4 nsecs from the bucket center. Chromaticity set to be $\xi = 4.0$, $\xi' = 1500$ and σ_τ= 3 necs.

As can be see in Fig. (6-7) this structural effect depends strongly on bunch intensity another clear sign that it is a wake field effect.

In this paper we will examine the effect of transverse wake fields and construct a model which combines the effects of linear, 2nd order chromaticity and resistive wall transverse wake field which reflects the behavior of the transverse collective motion of single coalesced bunch motion in the Tevatron.

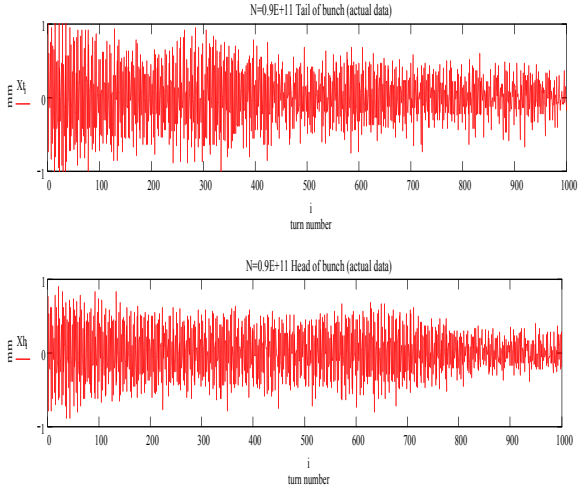

FIG. 6: Low Intensity bunch with $N_p = 0.9E{+}11$. Transverse beam motion after 1 mm kick with .4 nsec longitudinal bunch slices of Head (top) and the Tail (bottom) each 4 nsecs from the bucket center. Chromaticity measured to be $\xi = 4.0 \pm 1$ and σ_τ= 3 necs.

IV. THE EFFECT OF TRANSVERSE WAKE FIELDS

The inclusion of transverse wake fields in Eq. (3) requires the addition of a term on the right hand side which is the integral of the transverse motion of all particles 'ahead' of the current particle,

$$
-\frac{r_0}{C\gamma}\int_{-\infty}^{\infty}\int_{z}^{\infty} d\delta dz'\rho(z',\delta)Y(s,\delta,z')W_\perp(z-z'). \tag{13}
$$

Here $r_0 = e^2/m_0c^2$, C is the circumference of the ring, $W_\perp(z)$ is the transverse wake field, $N = \int dz'\rho(z')$ is the number of particles in a bunch.

We can recast the differential equation with the wake field driving term by using the solution we already found

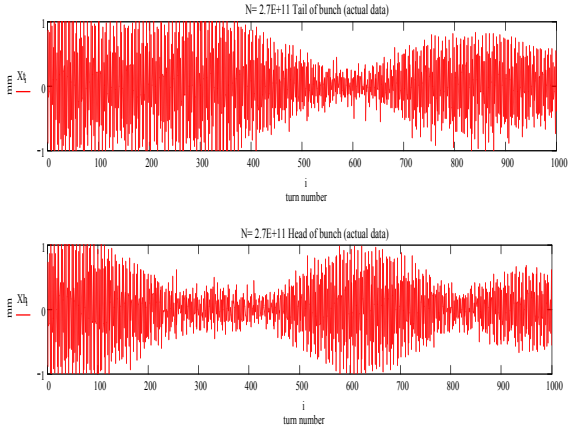

FIG. 7: High Intensity bunch with $N_p = 2.7E + 11$. Transverse beam motion after 1 mm kick with .4 nsec longitudinal bunch slices of Head (top) and the Tail (bottom) each 4 nsecs from the bucket center. Chromaticity measured to be $\xi = 4.0 \pm 1$ and σ_τ= 3 necs.

for the homogenous equation $Y = A\exp(-i\frac{\chi}{c}(z(s) - z(0))) + i\omega_\beta s/c)$ assuming A'' is small and again dropping all terms of the order Q^2 we can obtain a first order differential-integral equation,

$$\frac{dA}{ds} = i\alpha e^{i\frac{\chi}{c}z(1-\cos(\omega_s s/c))+i\delta\frac{\xi}{Q_s}\sin(\omega_s s/c)} \int_{-\infty}^{\infty}\int_{z}^{\infty} d\delta' dz' \rho(z',\delta')A(s,\delta',z') \times e^{-i\frac{\chi}{c}z'(1-\cos(\omega_s s/c))-i\delta'\frac{\xi}{Q_s}\sin(\omega_s s/c)} W_{0\perp}(z-z') \quad (14)$$

setting $\alpha = \frac{r_0 W_{1\perp} N c}{2\omega_\beta \gamma C}$ and using $\tau = z/c$. We have factored out the $W_{1\perp}$ the constant coefficient of the transverse wake field. This equation can be numerically integrated for any given number of macro-particles N_p, wakefield and initial distribution. We use a simple Euler step integrator method and step the amplitude using,

$$dA(z_{ip1}(n),n) = iw_r \sum_{ip2}^{N_p} A(z_{ip2}(n),n) e^{\frac{-i\chi}{c}(z_{ip1}(n)-z_{ip1}(0)-z_{ip2}(n)+z_{ip2}(0))} W_{0\perp}(z_{ip1}(n)-z_{ip2}(n)) \quad (15)$$

Here the wakefield is causal with $W_{0\perp}(x) = 0$ when $x > 0$ and $z_i(n) = r_i\cos(\phi_i(n))$ and the phase $\phi(n)$ is the synchrotron phase. A random Rayleigh distribution in r_i and uniform in $\phi(0)_i$ for N_p particles is used to develop a Gaussian distribution in τ and δ . We have also introduced w_r which is just $w_r = \alpha\frac{C}{Q_s\sqrt{\sigma_z}N_p}$, which is a combination of our integration time step, normalization and wake strength. At the end of each step integrate over δ or,

$$Ab(z,n) = \sum_{ip}^{N_p} A(z_{ip}(n),n) \times e^{\frac{-i\chi}{c}(z_{ip}(n)-z_{ip}(0))}\Theta(|z-z_{ip}(n)|-L) \quad (16)$$

Where L is the pickup length and $\Theta(x)$ the step function. We begin with Gaussian distribution of N_p particles in z. Using a resistive wall wake field of the form,

$$W_{0\perp}(z) = \frac{1}{\sqrt{z}}. \quad (17)$$

Integrating over 1000 turns we find that many of the asymmetric features of the evolution of the beam can be reproduced. A comparison between the simulation and actual beam motion is shown in Fig. 8 - 9.

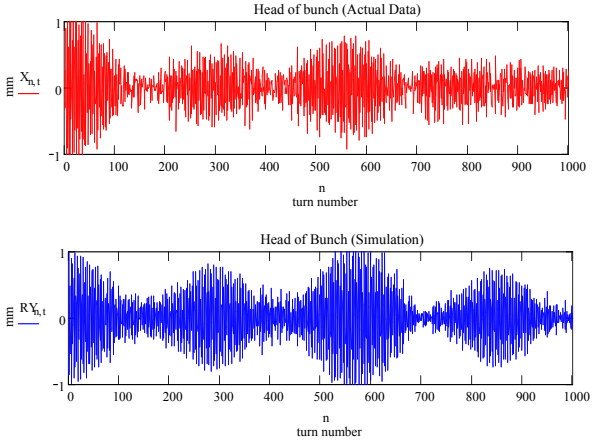

FIG. 8: Transverse (horizontal) turn-by-turn data of Head after a 1 mm kick 4 ns ahead of bucket center. Actual turn-by-turn data (top) compared with 1000 particle simulation with resistive wall wake $W_{1\perp} = 12cm^{1.5}$ and chromaticity $\xi = 3.733$ and $\sigma_\tau = 3$ nsecs.

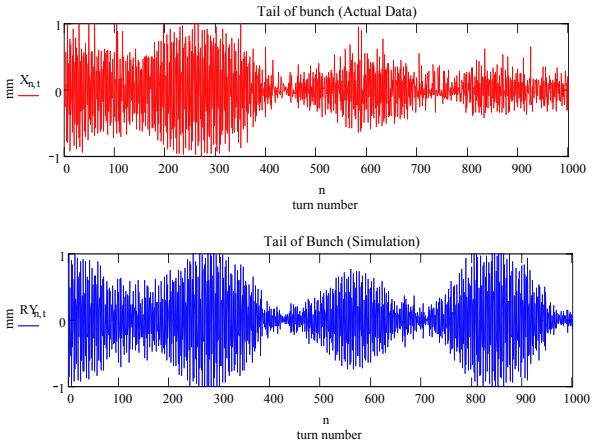

FIG. 9: Transverse (horizontal) turn-by-turn data of Tail after a 1 mm kick 4 ns behind bucket center. Actual turn-by-turn data (top) compared with 1000 particle simulation with resistive wall wake $W_{1\perp} = 12cm^{1.5}$ and chromaticity $\xi = 3.733$ and $\sigma_\tau = 3$ nsecs.

Although much of the structure of the beam envelope evolution has been captured by this simple model there remain a few significant discrepancies. Firstly the overall de-coherence time is not accurately represented by this model and secondly the envelope has significant mismatch at the center of the bunch as is shown in Fig. 10.

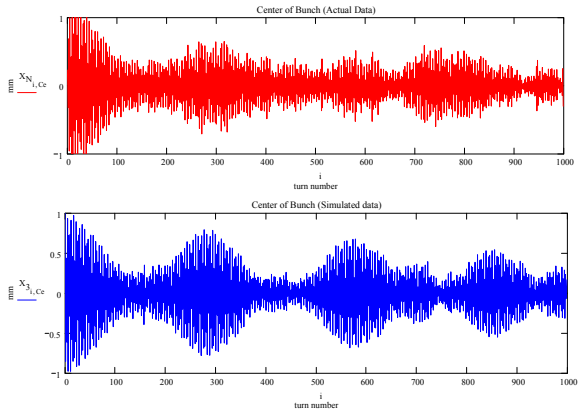

FIG. 10: Transverse (horizontal) turn-by-turn data of Center after a 1 mm kick 4 ns behind bucket center. Actual turn-by-turn data (top) compared with 1000 particle simulation with resistive wall wake $W_{1\perp} = 12cm^{1.5}$ and chromaticity $\xi = 3.733$ and $\sigma_\tau = 3$ nsecs.

V. EXTENDING MODEL TO 2ND ORDER CHROMATICITY

We now extend the model to include second order chromaticity. This leads to simple modification of Eq. (15) and Eq. (16) to include the phase terms given in Eq. (10).

$$z2_{ip1} = r_{ip1}^2\left(\frac{\phi_{ip1}}{2} - \frac{\sin(2\phi_{ip1})}{4}\right) \quad (18)$$

Here $z2_{ip1}$ is the 2nd order part of the phase and $\phi_{ip1} = \omega_s s/c + \phi$. So now Eq. (15) becomes,

$$dA(z_{ip1}(n), n) = iwr\sum_{ip2}^{N_p} A(z_{ip2}(n), n)e^{\frac{-i\chi}{c}(z_{ip1}(n)-z_{ip1}(0)-z_{ip2}(n)+z_{ip2}(0))} \times$$
$$e^{-i\frac{\chi_2}{c^2}(z2_{ip1}(n)-z2_{ip1}(0)-z2_{ip2}(n)+z2_{ip2}(0))}W_{0\perp}(z_{ip1}(n) - z_{ip2}(n)) \quad (19)$$

And Eq. (16) becomes,

$$Ab(z, n) = \sum_{ip}^{N_p} A(z_{ip}(n), n)e^{\frac{-i\chi}{c}(z_{ip}(n)-z_{ip}(0))}$$
$$\times e^{\frac{-i\chi_2}{c^2}(z2_{ip}(n)-z2_{ip}(0))}\Theta(|z - z_{ip}(n)| - L) \quad (20)$$

Here we define a second order head-tail phase ampli-

tude term, $\chi_2 = \frac{\omega_0 \omega_s \xi'}{2\eta^2}$. The results of simulations with 2nd order chromaticity and resistive wall wake field are shown in Fig. (11) where now with second order chromaticity of about 3000 we can account for both the decoherence time and the envelope structure at the bunch center.

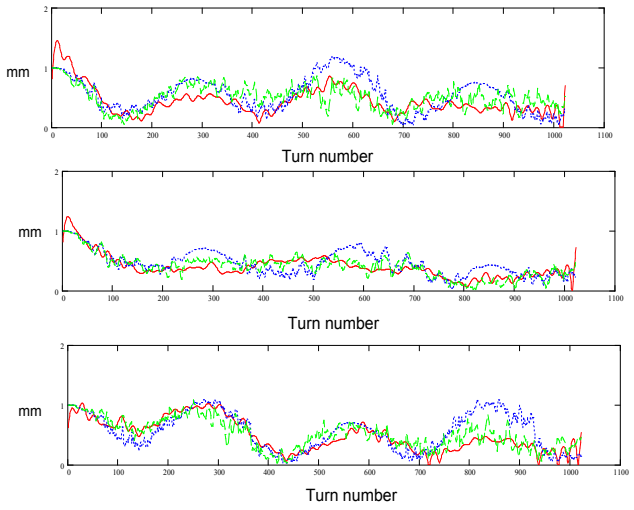

FIG. 11: Transverse (horizontal) envelope of turn-by-turn data of Head (top), Center (middle) and Tail (bottom) after a 1 mm kick. The head and tail are 4 ns away from the bucket center. Shown is the actual envelope data (red trace) overlaid with 1000 particle simulation with resistive wall wake $W_{1\perp} = 12cm^{1.5}$ and chromaticity $\xi = 3.733$ and σ_τ = 3 ns only (blue trace). Adding second order chromaticity of $\xi' = 3000$ (Green trace).

This level of 2nd order chromaticity compares with measured chromaticity on the order of 1500 units (measured on a separate occasion). Checking the vertical plane as can be seen in Fig. (12) the best fit yields -3400 units this compares with -1700 (measured on a separate occasion) for the measured values.

VI. INCLUSION OF SYNCHROTRON FREQUENCY SPREAD

Without too much difficulty it is possible to further extend our model to include the effective synchrotron frequency spread for particles oscillating in the outer part of the RF bucket. This effect can be approximated by allowing our phase to increment to shift with radial amplitude as,

$$\delta\phi_{ip} \approx -k_{rf}^2 r_{ip}^2/16. \tag{21}$$

The inclusion of this effect shifts the coherence temporal pattern on the outer edges of the bunch allowing an even better fit to our actual data as can be seen in Fig. (12). In this figure data from the vertical plane is

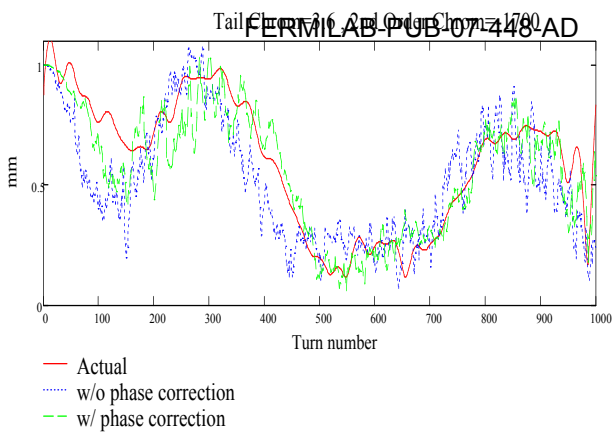

FIG. 12: The (vertical) transverse envelope of the turn-by-turn data for the Tail after a 1 mm kick. The tail is 4 ns away from the bucket center. The red trace is actual vertical data, blue simulation with resistive wall wake $W_{1\perp} = 19cm^{1.5}$, chromaticity $\xi = 3.7$, bunch length $\sigma_\tau = 3$ ns, second order chromaticity of $\xi' = -3400$ only. The green trace shows the effect of adding Eq. (21) correction to the synchrotron phase

shown. The fit is clearly improved with inclusion of 2nd order synchrotron frequency shift.

VII. FITTING BEAM PARAMETERS TO MODEL

With a model which appears to represent the main features of the longitudinally sliced wave form, an attempt can be made to use fits to the actual data to extract beam parameters. We accomplished these fits by pre-computing scans varying wake field strength, chromaticity and 2nd order chromaticity, then picking the minimum $\hat{\chi}^2$ value where we define,

$$\hat{\chi}^2 = \sum \frac{X_{meas} - X_{fit}}{X_{meas}}. \tag{22}$$

This approach does require significant computation time up front to generate the scans but once calculated can be reused to fit other data. We used a simple program written in mathcad but a short script should work as well. The actual fitting process required only a few minutes. In this way online computation of first and second order chromaticity with resistive wall strength is feasible.

Of course with this approach the resolution of the beam parameters is limited by the pre-computed parameter step size and range. Since current measurements of linear chromaticity typically have errors of about +/- 1 unit and 2nd order +/- 100 units we chose a step size of about 0.3 and 1000 which in terms of χ and χ_2 are both 0.1. We chose less precision for the 2nd order since we did not have any very accurate measurements of this value and

TABLE I: Horizontal fits to turn-by-turn data

T:CXINJ	N particles (E11)	$\xi_x \pm 1$	$\xi'_x \pm 1E3$	$W_{1x}(1/cm^{1.5})$	χ^2
Data Taken November 27 2003 (before liner install)					
33	< 1.11	3.425	4000	$19 >$	380
37	< 1.11	5.293	4000	$32 >$	400
39	< 1.11	5.604	4000	$38 >$	500
41	1.11	9.651	6000	58	600
37	2.26	6.227	5000	28	500
39	2.26	7.161	5000	30	400
41	2.26	9.028	6000	30	300
Data Taken April 15 2003 (before liner install)					
30	1.14	0.9	2000	30	300†
Data Taken August 22 2006 (after liner install)					
44	2.30	6	1000	12.5	400
42	2.30	4	1000	12.5	318
41	2.30	3.425	1000	12.5	212
40	2.30	2.5	0	12.5	254
39	2.30	2.179	0	12.5	216
Data Taken August 24 2006 (after liner install)					
39	2.44	1.8	1000	12	19
41	2.44	3.425	2000	12	38
42	2.44	4.67	3000	12	62
43	2.44	5.6	4000	12	300
44	2.44	8	0	16	600

for calculation time considerations. We processed several sets of data taken over a three year period of the Tevatron's life covering the period before the application the liner on the F0 lambertson magnet and after. Using our gross fitting method one can see in Table. I - II , if we ignore the outliers, an over all reduction in the strength of the transverse wake function coefficient for the resistive wall wake, falling from $30 - 12cm^{-1.5}$ in the horizontal plane and from $34 - 16cm^{-1.5}$ in the vertical. In terms of effective impedance this represents a reduction from $2.8 - 1.0M\Omega/m$ and $3.0 - 1.5M\Omega/m$ in the horizontal and vertical planes respectively (at 100 MHz) which is consistent with previous estimates of the impact of the liner [5] which claimed a reduction from $2.4 - 1M\Omega/m$.

We fit the central 10 points spanning $4nsec$ over 1000 turns, beyond 10 points the quality of the signal deteriorated with larger chromaticity. The fits depend on the level of linear chromaticity due to the fact that the signal to noise for the experiment would fall off with chromaticity. This is due to the nature of the chromaticity sextupole magnets whose contribution to 2nd order chromaticity increases with field strength. Thus with higher 2nd order chromaticity more damping was present. This increase in noise level was also present in the simulation, as 2nd order chromaticity and wake field strength were increase the noise of our results increased using only 1000 macro-particles. A higher number of macro-particles were needed to lower the noise levels of the simulation results and required longer simulation times. Due to time considerations we chose to use only 1000 macro-particles. This resulted in the quality of the fits falling off above 6 units of machine chromaticity. The useable signal across the bunch would fall off from the ends of the bunch as chromaticity increased. This had the general effect of blurring the effect of the short range wake with that of 2nd order chromaticity since the distinguishing features are evident in ends of the bunch. As a result those fits with chromaticity above 6 units would often settle in a false $\hat{\chi}^2$ minimum mixing 2nd order chromatic effects with wake field and vice versa. On the lower end of the chromaticity values this problem of distinguishing 2nd order chromaticity from short range wake field effects was evident due to the fact that a very small level of 2nd order chromaticity can 'look like' the effects of a short range wake field. This problem can be seen reflected in our data as an under-valuing of the short range wake field strength at low chromaticities and over-valuing for high chromaticities.

The data set taken on April 15th also had problems due to the fact that the horizontal chromaticity was not kept constant and it is unclear what impact the high horizontal chromatic sextupole would have on 2nd order chromaticity in the vertical plane. Since we only fit the beam envelope it would seem that fitting the phase may help above 6 units of chromaticity and minimize the effect of the redundant minimums. An examination of data with chromaticites greater than 6 units revealed discrepancies in the phase which if fit would yield a more consistent valuation of the linear chromatic values.

TABLE II: Vertical fits to turn-by-turn data

T:CYINJ	N particles (E11)	$\xi_y \pm 1$	$\xi'_y \pm 1E3$	$W_\perp\,(1/cm^{1.5})$	χ^2
Data Taken April 15 2003 (before liner install)					
33	1.59	11	−7666	40.7	1107
35	1.61	8.7	−5000	40.2	668
31.5	1.26	5	−5000	44	571
28	1.00	2.4	1000	29	181
28	1.80	2.4	−1000	24	320
28	1.85	3.3	−4000	33	394
28	0.86	2.1	−4000	34	628
30	1.69	3.3	−4000	18	353
26	1.82	1.2	−2000	12	229
32	1.87	8.7	−5000	35	655
Data Taken August 24 2006 (after liner install)					
25	2.55	5	−4000	25	626
24	2.55	4.35	−3000	19	517
23	2.55	3.425	−3000	16	398
22	2.55	2.802	−2000	16	610
22.5	2.55	3.425	−2000	19	578

Our experience suggests that the best approach to apply this method would be to first independently measure linear and second order chromaticity and then fit the wake field coefficient. Or conversely once the strength of the short range wake field is determined to fit linear and 2nd order chromaticity.

VIII. CONCLUSION

Using a simple multi-particle simulation we have been able to recover the outstanding features of the single bunched beam evolution after the application of a kick. Comparisons with this model allowed us to fit both the strength of the associated wake field due to resistive wall and deliver values for the 1st and 2nd order chromaticity. Using a database of pre-computed scans can permit the possibility of fitting either all three parameters, linear chromaticity, 2nd order chromaticity and resistive wall wake field strength, or more accurately measuring two or more parameters and fitting the third for a robust method of measuring the relevant beam parameters during operation.

IX. ACKNOWLEDGMENTS

We are particularly grateful to Alexey Burov for supplying me with his basic Head-tail code which is the basis used to develop the simulations shown here. Also for his advice and going over the manuscript.

[1] P. M. Ivanov et. al, Proc. of PAC2003, Portland, Or, p.3062.
[2] P. M. Ivanov et. al, Proc. of PAC2005, Knoxville, Tn p.1714
[3] S. Fartoukh and R. Jones, LHC Project Report 602 (2002).
[4] A. W. Chao "Physics of Collective Beam Instabilities in High Energy Accelerators", John Wiley and Sons, NY pp 147-149 (1993).
[5] P. M. Ivanov, F0 Lambertson liner review (2003), internal FNAL document.